Proceedings of the 7th World Congress on Momentum, Heat and Mass Transfer (MHMT'22)
~~Lisbon, Portugal~~ Virtual Conference – April 07 – 09, 2022
Paper No. ICMFHT 141
DOI: 10.11159/icmfht22.141

Gas-Liquid Flow Regime Variation along a Pipeline Riser

Alexander J Elliott[1*], Graeme Hunt[1], Andrea Cammarano[1], Gioia Falcone[1]
[1]James Watt School of Engineering, University of Glasgow
Glasgow, G12 8QQ, United Kingdom
Alexander.Elliott@glasgow.ac.uk; Graeme.Hunt@glasgow.ac.uk; Andrea.Cammarano@glasgow.ac.uk;
Gioia.Falcone@glasgow.ac.uk

Abstract
This paper presents the initial findings of a study into the development of gas-liquid flows as they pass through a catenary-style pipeline riser, similar to those utilised in the oil and gas industry. A commercial, one-dimensional multiphase flow software (PETEX GAP) is used to scope two test points that represent flow regimes that are likely to occur in such a system. These test points are explored further using computational fluid dynamics, calculated using StarCCM+. In both test points, the gradient of the riser is observed to accelerate the onset of Kelvin-Helmholtz waves. Depending on the flow rates, these waves can lead to several interesting flow phenomena, such as the initiation of sloshing and the occurrence and dissipation of slug flow. The potentially destructive nature of these effects is explored, particularly in terms of the implications for experiments using flexible risers, as well as industrial pipelines of this form.

***Keywords*: multiphase flow, pipeline riser, flow regimes**

1. Introduction

Two-phase, gas-liquid flows are frequently observed in a variety of industrial processes, including sewage systems, power plants, and, of greatest relevance to the present work, oil and gas pipelines. Depending on the operating conditions of the system, the flow may fall into one of several regimes, some of which can lead to large-scale mechanical failure (Farghaly, 1987). Therefore, the ability to model and predict these flow patterns, as well as how they may change and develop with changes in conditions, remains an active area of research.

The orientation of a pipe is a major factor in defining the flow regime, as has been thoroughly investigated through analytical models. This was initially explored for horizontal pipes (Wallis & Dobson, 1973), (Bendiksen & Espedal, 1992), and was expanded to investigate pipes with slight inclination (Dukler & Hubbard, 1975), (Taitel & Dukler, 1976). The flow pattern maps defined in (Taitel & Dukler, 1976) are observed to vary when the inclination is increased from 1° to 5°, with the transition boundary between flow regimes occurring at higher gas and liquid superficial velocities in the latter case. This is consistent with the noticeably different boundary transitions calculated for vertical flows (Taitel, Bornea, & Dukler, 1980), (McQuillan & Whalley, 1985). A key focus of the aforementioned papers is the investigation of flow pattern transition mechanisms, whether this be the onset of slugging in horizontal flow (Vaze & Banerjee, 2010), (Sergeev, Vatin, Kotov, Nemova, & Khorobrov, 2020), or the transition between plug and churn flow in a vertical riser (McQuillan & Whalley, 1985), (Montoya, Lucas, Baglietto, & Liao, 2016). Despite the clear influence that the pipe orientation has on flow regimes and transitions, the studies in the literature focus almost entirely on straight channels, rather than curved pipes.

As the global energy system transitions to renewable sources, the use of traditional fuels remains crucial in maintaining energy security. This necessitates the exploitation of increasingly complex oil fields, which require complex riser geometries, including S-shaped (Li, Guo, & Li, 2013) and catenary risers (Duan, Chen, You, & Gao, 2017), (Qi., Gao, & Guo, 2019), (Jørgensen, Tonnesen, & Mandø, 2020). Although research in this area continues to expand, the focus has been placed solely on the occurrence of severe slugging, a specific case of the slug flow regime, in which the liquid slug fills the full riser pipeline. The study presented in this paper aims to expand this research by considering the development

[*] Now at Cranfield University (Alex.J.Elliott@cranfield.ac.uk)

of several flow regimes along catenary-style risers. The work was initiated to aid the development of an experimental campaign for the MUFFINS project (2019), which focuses on the occurrence of fluid-structure interactions for flexible pipeline risers exhibiting slug flow. In this initial study, a number of non-slugging cases are considered, so that a wider understanding of the physics may be obtained. Moreover, a rigid system is assumed, so that the influence of the on the flow regime may be considered in isolation. The test points are first scoped using the Petroleum Experts (PETEX) General Allocation Package (GAP), before being explored in more detail using computational fluid dynamics (CFD).

2. Pipeline Riser Model

2.1. System overview

The aim of this work is to assess the development of water-gas flow regimes along a gradual pipeline riser, but the model begins with a 10 m horizontal section, which ensures that the flow is fully-developed as it reaches the riser section. This is followed by the riser section, which is represented as a quarter ellipse, with a horizontal major axis of length 7.6 m and vertical minor axis of length 5 m. The full length of the riser section is 10 m. A schematic for this system is given in Figure. Across the full pipeline (horizontal and riser), the internal diameter is maintained at 50.8 mm (2 in).

The inlet boundary is defined by a division into an upper and lower semi-circle, as this mimics stratified conditions achieved downstream of the mixing joint. The upper half is assumed to be pure Nitrogen, while the lower half is entirely made up of water. A constant pressure is assumed at the outlet at the top of the riser. The system is pressurised to 10 barg.

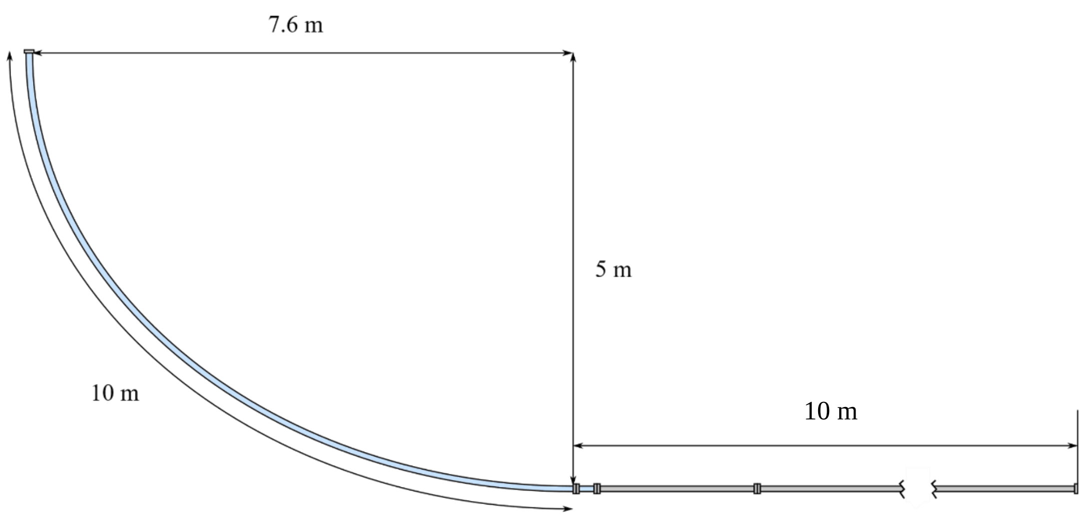

Figure 1: Schematic for the pipeline riser system.

2.2. One-dimensional modelling

The initial insight into the riser model is provided by a one-dimensional model developed using PETEX GAP This software is a multiphase flow simulator, originally designed to model oil and gas production and injection networks, but also has capabilities for modelling water-gas flow. The one-dimensional simulations provided by this software allowed a wide number of test points (TPs) to be considered, with the most suitable and interesting points for the MUFFINS project to be considered in further detail using StarCCM+.

Following a provisional scoping exercise using GAP, the following TPs have been identified for the 10 m horizontal section:

Table 1: Final TPs selected for further investigation.

Reference	Flow regime	u_{sg} (m/s)	u_{sl} (m/s)
TP1	Annular	10.11	0.28

TP2	Wavy	1.35	0.094

3. Computational fluid dynamics (CFD) model

This section outlines the application of the techniques used in the development of CFD slug flow time histories, along with the motivation for their use. This section outlines the application of the techniques used in the development of CFD slug flow time histories, along with the motivation for their use.

3.1. Volume of fluid model

The VOF model was developed using the assumption that the flow contains two or more fluids that are not interpenetrating. In practical terms, this means that, for each cell generated as part of the mesh in STAR-CCM+, the associated properties are functions of the phase fractions. Therefore, the continuity equations take the form

$$\partial_t \alpha_g + \nabla \cdot \left(\alpha_g \vec{u}\right) = 0, \tag{1}$$

$$\partial_t \alpha_l + \nabla \cdot (\alpha_l \vec{u}) = 0, \tag{2}$$

where α_g and α_l denote the gas and liquid volume fractions, and $\vec{u}$ is the single velocity field. To develop the momentum equation for the VOF model, it is assumed that the effective density and viscosity are calculated as linear combinations of the liquid and gas phase properties, so that $\rho = \alpha_g \cdot \rho_g + \alpha_l \cdot \rho_l$ and $\mu = \alpha_g \cdot \mu_g + \alpha_l \cdot \mu_l$, where ρ and μ denote the density and viscosity, respectively. Then, the momentum balance can be expressed in conservative form as

$$\partial_t \rho \vec{u} + \nabla \cdot (\rho \vec{u} \vec{u}) = -\nabla p + \nabla \cdot \tau + \rho \cdot \vec{g} + \rho \cdot \vec{F}. \tag{3}$$

Here, $\tau = \mu \cdot \left(\nabla \vec{u} + \nabla \vec{u}^{\mathrm{T}}\right)$ denotes the deviatoric stress tensor, p denotes the pressure, and

$$F = \sigma_{ij} \cdot \frac{\kappa_i \cdot \nabla \alpha_i}{\frac{1}{2}\left(\rho_i + \rho_j\right)} \tag{4}$$

denotes the interfacial surface tension between phases. In this equation, i and j represent the two phases, σ_{ij} is the surface tension coefficient, and κ_i is the curvature of the interface at the point of calculation.

3.2. The $\mathbf{k} - \boldsymbol{\varepsilon}$ turbulence model

Given that a stated aim of this work is to generate accurate predictions with minimal computational effort, the $k - \varepsilon$ turbulence model has been used to simulate turbulent flow conditions. Its compromise between computation time and accuracy has led to its wide application, both in industry and academia. As this is a semi-empirical scheme, Reynolds decomposition is applied to various fields, which are decomposed into a large, averaged term and a fluctuation term. These Reynolds decompositions take the form $\vec{\psi} = \bar{\psi} + \vec{\psi}'$. Therefore, an additional set of two conservations are required to calculate the Reynolds stresses, the first for the turbulent kinetic energy, k, and the second for the rate of turbulence dissipation, ε. These two equations are written as

$$\partial_t \rho \cdot k + \nabla \cdot (\rho \vec{u} k) = \nabla \cdot \left(\left(\mu + \frac{\mu_t}{\sigma_k} \right) \nabla k \right) + G_k - \rho \cdot \varepsilon, \tag{5}$$

$$\partial_t \rho \cdot \varepsilon + \nabla \cdot (\rho \vec{u} \varepsilon) = \nabla \cdot \left(\left(\mu + \frac{\mu_t}{\sigma_\varepsilon} \right) \nabla \varepsilon \right) + C_1 \cdot \frac{\varepsilon}{k} \cdot G_k + C_2 \cdot \rho \cdot \frac{\varepsilon^2}{k}. \tag{6}$$

Here, σ_k, σ_ε, C_1, and C_2 are empirical constants. μ_t denotes the turbulent viscosity, derived from k and ε, calculated as

$$\mu_t = \rho \cdot C_\mu \cdot \frac{k^2}{\varepsilon}, \tag{7}$$

where $C_\mu \approx 0.09$ is an experimental constant.

Finally, the source term of turbulence – denoted G_k – is defined in terms of both the turbulent viscosity and the velocity gradients, and is expressed as

$$G_k = \mu_t \cdot (\nabla \bar{u} + \nabla \bar{u}^{\mathrm{T}}) \cdot \nabla \bar{u}^{\mathrm{T}} - \frac{2}{3} k \cdot \nabla \bar{u}. \tag{8}$$

The computational process for this model begins by solving the transport equations for k and ε, which can then be applied in the calculation of the turbulent viscosity. The Reynolds stresses are computed and substituted into the momentum equations. Through these steps, the velocity is recalculated, and its components are used to update G_k. The full time history is generated through the repetition of these steps.

4. Results and discussion

This section investigates the development of the flow regime along a graduated riser for the test points listed in Table 1.

4.1. Test Point 1 (TP1)

TP1 was defined to have superficial velocities of $u_{sg} = 10.11$ m/s and $u_{sl} = 0.28$ m/s. The flow regime predicted by GAP for the horizontal region was annular. However, the flow observed in the 60 s StarCCM+ simulation exhibited stratified wavy flow characteristics, as can be observed in Figure 2a; the reason for this discrepancy was unclear, but may be a result of the collapse of the inlet stratified flow condition at half channel height to the observed stratified water level of less than a quarter channel height. As the Kelvin-Helmholtz waves pass through the riser, they grow in height, from a normalised of height of ~0.25 in the horizontal development section (Figure 2a) to ~0.4 in the early sections of the riser (Figure 2b-c). As the waves approach the midpoint of the riser, they begin to lose some of their definition, either collapsing or initiating a sloshing effect. The breakup of the waves and sloshing can be particularly observed in the right-hand side of the riser in Figure 2c, and is explored for the mid-riser in Figure 4 and Figure 4.The waves presented in Figure 2a are approximately equal in heigh and occur pseudo-periodically. In Figure 2b, these single-peaked waves begin to lose definition, before becoming disordered in the mid-riser (Figure 2c). It is theorised that this breakup is a result of the relative contribution of the gravity force increasing as the gradient of the riser approaches the vertical orientation.

Figure 4 also demonstrates that, in some of these waves, parts of the liquid can become completely detached from the main flow. The blue boxes in Figure Figure 4 also present evidence for the aforementioned sloshing effect; specifically, the water volume fraction (VF) is notably higher at the walls than at the centre. This trend becomes more pronounced in the later riser, as presented in Figure 5. In view (a), it can be observed that the VF is less than 0.4 throughout and less than 0.1 in the majority of the channel. In contrast, view (b) demonstrates that the VF is between 0.5 and 1.0 for a large proportion of the riser section. Finally, Figure 6 provides insight into the mechanism through which the sloshing in the mid-riser can lead to an annular style flow pattern in the upper sections. Specifically, once the sloshing wave reaches a certain height, the water continues moving around the perimeter, leaving a column of gas in the centre. Although not presented here, the flow regime in the vertical section can be categorised as fully annular, with some occurrences of churn-like behaviour. The sloshing behaviour observed in the riser for TP1 may have important implications for a flexible riser, potentially leading to out-of-plane vibrations that may not occur for other flow regimes.

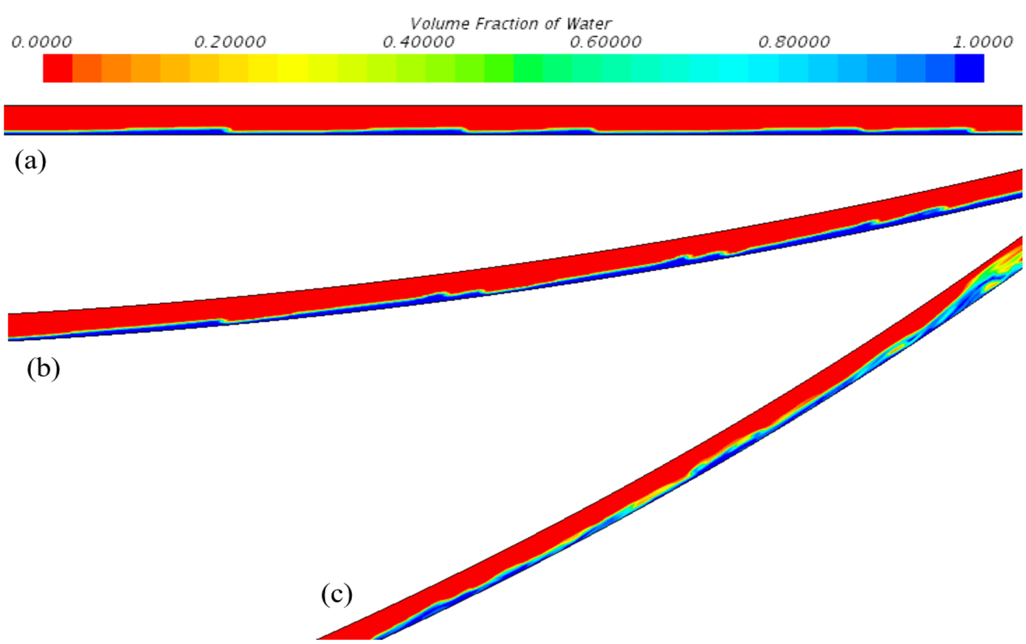

Figure 2: Development of Kelvin-Helmholtz waves in the (a) horizontal section, (b) early riser, (c) early-mid riser, for TP1.

4.2. Test Point 2 (TP2)

As with TP1, there is a discrepancy between the TP2 horizontal flow regime ($u_{sg} = 1.35$ m/s, $u_{sl} = 0.094$ m/s) predicted by GAP and observed in the simulations; the behaviour was still observed to be stratified, but was smooth rather than wavy, as presented in Figure 7a. In Figure 7b, the rapid development of Kelvin-Helmholtz waves can be observed, leading to a much higher wave frequency than is observed for TP1. Furthermore, where these waves collapsed or transitioned to sloshing in TP1, the waves appear to coalesce for TP2, leading to slug or pseudo-slug flow, as can be seen in the right-hand side of the pipe in Figure 7c.

Figure 8 outlines the progression of these slugs as they enter the later stages of the riser. The figure shows that the liquid slug enters the mid-riser filled with gas bubbles, as indicated by the sections with VFsin the range 0-0.75; this has been confirmed through consideration of the slices used above, though these are omitted here for brevity. As the slugs continues through the riser, it becomes filled almost entirely with liquid (VF> 0.9) as the gas bubble dissipate up the riser. Given that the top of the presented section sees a much lower amount of liquid flow (again, verified with slice views), and that a band of VF = 1.0 can be observed to move downward, it can be concluded that there must be a backflow effect. Further, through consideration of the full time history, this series of behaviour is observed to occur periodically.

Finally, although not presented here, the late riser section was observed to be almost entirely gas throughout. This adds further confirmation of the outlined backflow effects.

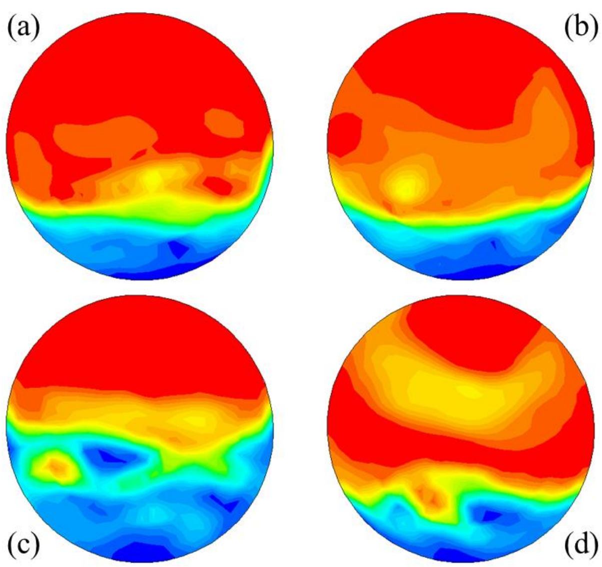

Figure 3: Mid-riser slice at times (a) 51.3 s, (b) 51.35 s, (c) 51.4 s, (d) 51.45 s, showing collapse and break up of Kelvin-Helmholtz waves.

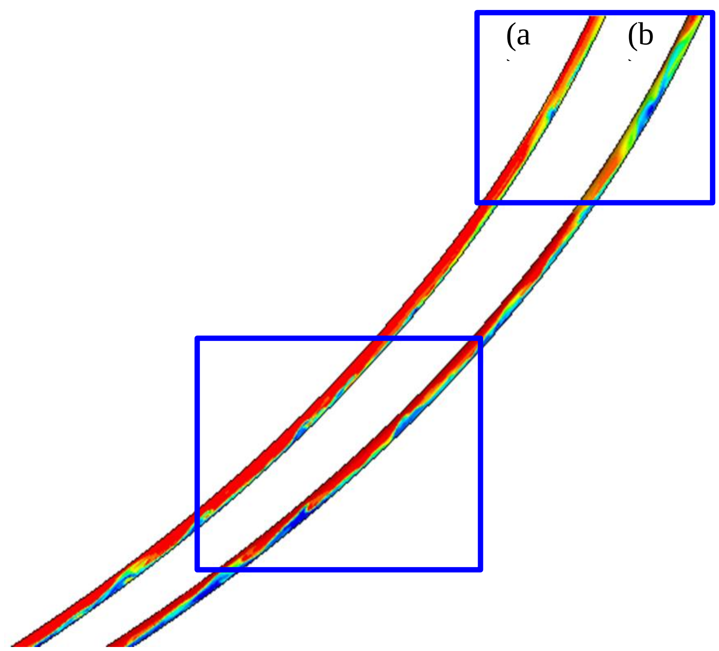

Figure 4: Development of the flow along the mid-riser for the (a) central slice and (b) outer wall of the pipe.

Figure 5: Development of the flow along the late riser for the (a) central slice and (b) outer wall of the pipe.

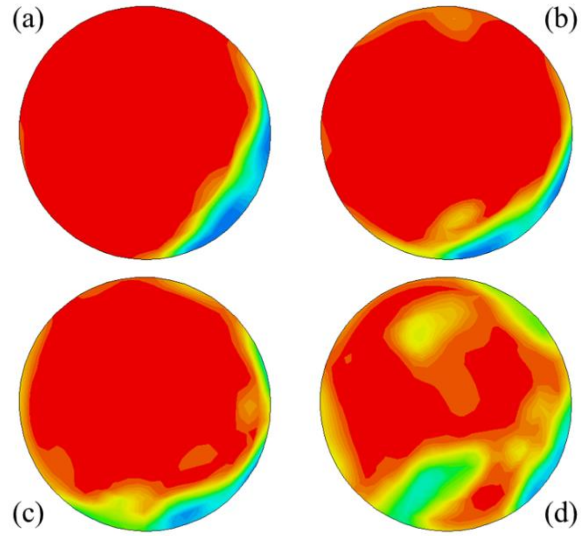

Figure 6: Late riser slice at times (a) 44.15 s, (b) 44.2 s, (c) 44.25 s, (d) 44.3 s, showing collapse and break up of Kelvin-Helmholtz.

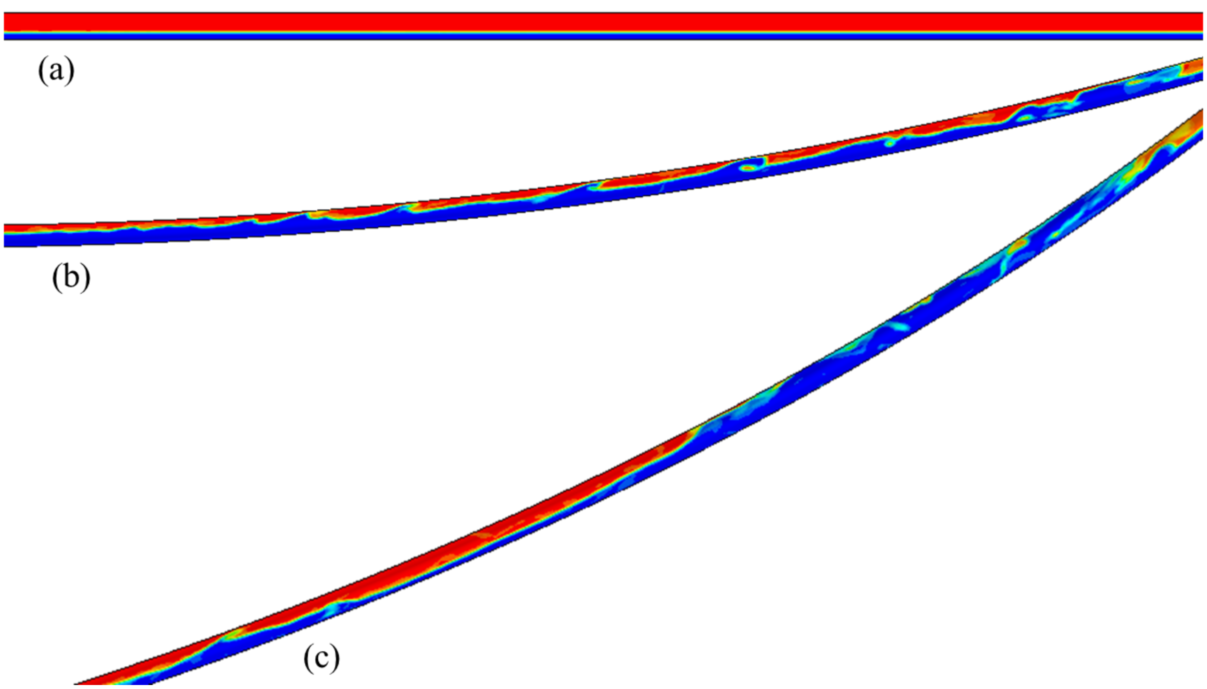

Figure 7: Development of Kelvin-Helmholtz waves in the (a) horizontal section, (b) early riser, (c) early-mid riser, for TP2.

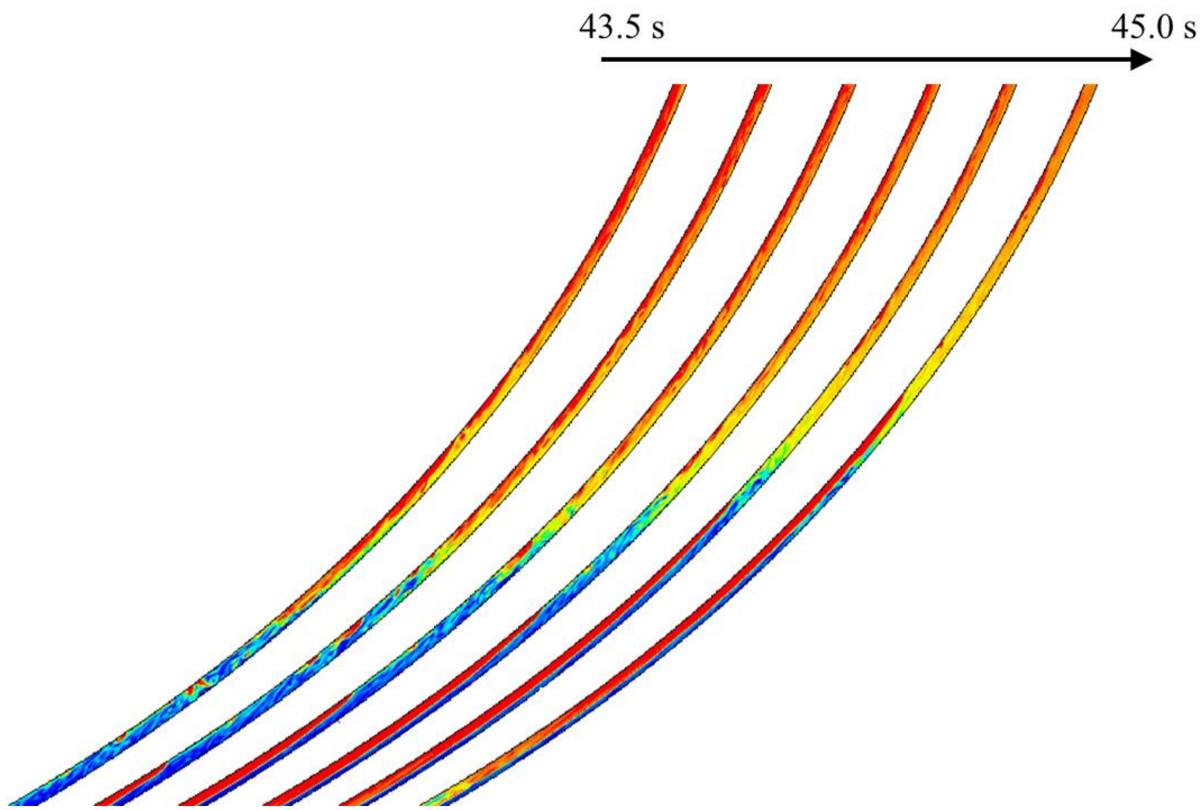

Figure 8: Development of liquid slug in mid-riser for TP2.

5. Conclusion

This paper presents the initial results from a wider investigation into the development of flow regimes along a catenary-style riser. Two methods were used to evaluate the TPs: the PETEX GAP software, and computational fluid dynamics, simulated using StarCCM+. Two TPs were selected, one with a stratified wavy flow pattern in the horizontal development section, the other with stratified smooth. In both cases, a number of interesting observations were made regarding the influence of the riser geometry on the development of the flow regime. In particular, the increasing gradient of the riser section was seen to accelerate the onset and development of Kelvin-Helmholtz waves, with these going to collapse due to backflow effects in higher sections of the pipeline. In addition, in TP1, these waves induced a sloshing behaviour that accelerated the progression to annular flow; the pseudo-periodic nature of this sloshing may have implications for the structural integrity of riser systems, particularly if the frequency is close to that of the natural frequencies of the pipeline. For TP2, the rapid onset of waves led to their coalescence, forming larger slugs, which represents another flow feature that is potentially harmful. The results summarised here have been developed to aid the design of the experimental component of the MUFFINS project and will be explored further when the experiments are completed.

Acknowledgements

The authors are grateful for the funding support from the Engineering and Physical Sciences Research Council (EPSRC) of UK Research and Innovation through the “MUltiphase Flow-induced Fluid-flexible structure InteractioN in Subsea applications (MUFFINS)” project grant EP/P033148/1.

References

[1] Bendiksen, K., & Espedal, M. (1992). Onset of slugging in horizontal gas-liquid pipe flow. *International Journal of Multiphase Flow*, *18*(2), 237-247.

[2] Duan, J.-L., Chen, K., You, Y.-X., & Gao, S. (2017). Experimental and Computational Investigations on Severe Slugging in A. *China Ocean Engineering*, *31*(6), 653-664.

[3] Dukler, A. E., & Hubbard, M. G. (1975). A Model for Gas-Liquid Slug Flow in Horizontal and Near Horizontal. *Industrial & Engineering Chemistry Fundamentals*, *14*(4), 337-347.

[4] Farghaly, M. A. (1987). Study of Severe Slugging in Real Offshore Pipeline Riser-Pipe System. *Paper presented at the Middle East Oil Show, Bahrain*.

[5] Jørgensen, R. T., Tonnesen, G. R., & Mandø, M. (2020). Comparative Study of CFD and LedaFlow Models for Riser-Induced Slug Flow. *Energies*, *13*, 3733.

[6] Li, N., Guo, L., & Li, W. (2013). Gas–liquid two-phase flow patterns in a pipeline–riser system with an S-shaped riser. *International Journal of Multiphase Flow*, *55*, 1-10.

[7] McQuillan, K. W., & Whalley, P. B. (1985). Flow patterns in vertical two-phase flow. *International Journal of Multiphase Flow*, *11*(2), 161-175.

[8] Montoya, G., Lucas, D., Baglietto, E., & Liao, Y. (2016). A review on mechanisms and models for the churn-turbulentflow regime. *Chemical Engineering Science*, *141*, 86-103.

[9] MUFFINS Project. (2019). Retrieved January 15, 2021, from MUFFINS Research Project: https://www.muffinsproject.org.uk/

[10] Qi., X.-L., Gao, S., & Guo, H.-Y. (2019). Numerical Investigation on Severe Slugging in A Catenary Riser. *China Ocean Engineering*, *33*(5), 628-635.

[11] Sergeev, V., Vatin, N., Kotov, E., Nemova, D., & Khorobrov, S. (2020). Slug Regime Transitions in a Two-Phase Flow in. *Applied Sciences*, *10*, 8739.

[12] Taitel, Y., & Dukler, A. E. (1976). A model for predicting flow regime transitions in horizontal and near forizontal gas-liquid flow. *AIChE Journal*, *22*(1), 47-55.

[13] Taitel, Y., Bornea, D., & Dukler, A. E. (1980). Modelling flow pattern transitions for steady upward gas-liquid flow in vertical tubes. *AIChE Journal*, *26*(3), 345-355.

[14] Vaze, M. J., & Banerjee, J. (2010). Experimental visualization of two-phase flow patterns and transition from stratified to slug flow. *Proceedings of the Institution of Mechanical Engineers, Part C: Journal of Mechanical Engineering Science*, *225*, 382-389.

[15] Wallis, G. B., & Dobson, J. E. (1973). The onset of slugging in horizontal stratified air-water flow. *International Journal of Multiphase Flow*, *1*, 173-193.